AGU PUBLICATIONS

Geophysical Research Letters

RESEARCH LETTER
10.1002/2016GL072148

Key Points:
- Method to find new low-frequency earthquake (LFE) templates
- Triggered and ambient tremor share a common source
- LFEs and therefore tremor locate on the deep extension of the Chaochou-Lishan Fault

Supporting Information:
- Supporting Information S1

Correspondence to:
A. C. Aguiar,
aguiar@llnl.gov

Citation:
Aguiar, A. C., K. Chao, and G. C. Beroza (2017), Tectonic tremor and LFEs on a reverse fault in Taiwan, *Geophys. Res. Lett.*, *44*, 6683–6691, doi:10.1002/2016GL072148.

Received 30 NOV 2016
Accepted 3 MAR 2017
Published online 6 JUL 2017

Tectonic tremor and LFEs on a reverse fault in Taiwan

Ana C. Aguiar[1,2], Kevin Chao[3], and Gregory C. Beroza[2]

[1]Lawrence Livermore National Laboratory, Livermore, California, USA, [2]Geophysics Department, Stanford University, Stanford, California, USA, [3]Center for Optimization and Statistical Learning, Northwestern Institute on Complex Systems, Northwestern University, Evanston, Illinois, USA

Abstract We compare low-frequency earthquakes (LFEs) from triggered and ambient tremor under the southern Central Range, Taiwan. We apply the PageRank algorithm used by Aguiar and Beroza (2014) that exploits the repetitive nature of the LFEs to find repeating LFEs in both ambient and triggered tremor. We use these repeaters to create LFE templates and find that the templates created from both tremor types are very similar. To test their similarity, we use both interchangeably and find that most of both the ambient and triggered tremor match the LFE templates created from either data set, suggesting that LFEs for both events have a common origin. We locate the LFEs by using local earthquake *P* wave and *S* wave information and find that LFEs from triggered and ambient tremor locate to between 20 and 35 km on what we interpret as the deep extension of the Chaochou-Lishan Fault.

1. Introduction

Taiwan is located between two major subduction zones. To the northeast, the Philippine Sea Plate subducts under the Eurasian Plate forming the Ryukyu arc system, and to the south, the South China Sea of the Eurasian Plate subducts under the Philippine Sea Plate at the Manila Trench [*Shin and Teng*, 2001; *Yu et al.*, 1997]. The island is divided into several north-northeast trending geologic provinces, and the Central Range province is part of this complex arc-continent collision environment [*Wu et al.*, 2016; *Yu et al.*, 1997].

Taiwan is also one of the places where tectonic tremor has been observed [*Peng and Gomberg*, 2010], but the tremor source is not well understood. Initially, tectonic tremor was associated with slow slip events in subduction zones such as in Cascadia, Japan, Costa Rica, and Alaska [*Brown et al.*, 2005; *Obara and Hirose*, 2006; *Peterson and Christensen*, 2009; *Rogers and Dragert*, 2003]; however, it was subsequently discovered in different tectonic regimes including the San Andreas Fault [*Nadeau and Dolenc*, 2005]. Tectonic tremor can occur spontaneously or be triggered by the strong shaking from distant large earthquakes [*Gomberg et al.*, 2008]. Examples include the 2003 M_w 8.1 Tokachi-oki that triggered deep low-frequency earthquakes (LFEs) [*Miyazawa and Mori*, 2005]; the 2012 M_w 8.6 Sumatra earthquake, which triggered widespread tremor in the subduction zone and inland fault active regions in Japan [*Chao and Obara*, 2016]; and the 2002 M_w 7.8 Denali, Alaska earthquake, which triggered tremor on Vancouver Island, British Columbia [*Rubinstein et al.*, 2007] as well as throughout California [*Gomberg et al.*, 2008]. This is also the case for Taiwan, where tectonic tremor was first observed under the southern Central Range, triggered by the Love waves from the 2001 M_w 7.8 Kunlun earthquake in northern Tibet [*Peng and Chao*, 2008]. Triggered tremor in Taiwan was subsequently observed during the passage of waves from a series of teleseisms [*Chao et al.*, 2012; *Chao et al.*, 2013a; *Tang et al.*, 2010], with evidence for triggered tremor below the northern Central Range as well [*Chao et al.*, 2013a].

Tang et al. [2010] demonstrated that triggered tremor in Taiwan is composed of LFEs. LFEs were originally found manually by *Katsumata and Kamaya* [2003] in Japan, and later shown to constitute tectonic tremor when occurring as a swarm [*Brown et al.*, 2009; *Ide et al.*, 2007; *Shelly et al.*, 2007b, 2006]. In Taiwan, LFEs were originally identified manually, but following a match-filter technique by cross-correlating the signal of the known LFEs with tremor [*Shelly et al.*, 2007a, 2007b], these signals were later used as templates to detect more triggered LFEs [*Tang et al.*, 2010, 2013]. With this method, they were able to locate LFEs within tremor under the Central Range, close to the downward extension of the steeply dipping Chaochou-Lishan Fault. More recent studies show that tremor in Taiwan is not only triggered but also occurs spontaneously [*Idehara et al.*, 2014; *Sun et al.*, 2015]. These episodes, denoted as ambient tremor, have also been reported under the southern Central Range and locate to a similar area as the triggered tremor [*Chao et al.*, 2013a; *Chuang et al.*, 2014].

Even though some studies locate the tremor bursts under the southern Central Range close to the Chaochou-Lishan Fault [*Tang et al.*, 2010], there are other studies that suggest that tremor may be a result of subduction [*Ide et al.*, 2015]. Large location uncertainties have left it unclear whether the downward extension of the Chaochou-Lishan Fault or subduction of the Eurasian plate is the tremor source region. In this study we focus on analyzing LFEs within tremor in Taiwan by using PageRank as an earthquake detection method [*Aguiar and Beroza*, 2014] to find LFEs during both triggered and ambient tremor without a priori knowledge of LFE waveforms. We compare LFEs found from both data sets and use local earthquakes to find the *P* wave signal of the LFEs to aid in the location of the events.

2. PageRank Applied to Tremor in Taiwan

We first perform an initial cross correlation on all windows following *Brown et al.* [2008] and later use an adaptation of Google's PageRank algorithm [*Page et al.*, 1999] to find directly and indirectly linked windows that comprise robust LFEs. We focus on windows with high PageRank values and stack all other windows linked, both directly and indirectly, to the highly ranked window to create templates following *Aguiar and Beroza* [2014]. Once templates are established, we use them to search continuous data by template matching. To find new detections we perform the analysis on each station/component independently and associate all stations by comparing all detections within a 2 s window. We associate all stations and declare a window a detection if that window is found in the total number of stations that gives us a probability of finding one false detection in 1000 based on binomial statistics. We apply the method to both triggered and ambient tremor and create LFE templates for both independently, without a priori knowledge of the template signature in both cases.

2.1. Ambient Tremor

Ambient tremor bursts are ongoing in Southern Taiwan [*Chao et al.*, 2013b]; we begin our analysis by selecting 1 day (19 January 2009) with a clear 30 min tremor episode (Figure 1a).

We band-pass filter the data between 4 and 8 Hz and use a 10 s window for the initial cross correlation. This is a narrower frequency band than the typical 1–8 Hz used in other areas; however, narrow bandwidth tremor is also observed in Guerrero, Mexico (1–2 Hz) [*Frank and Shapiro*, 2014; *Frank et al.*, 2013; *Payero et al.*, 2008] and in the Hikurangi subduction zone, in northern New Zealand [*Kim et al.*, 2011]. We perform a cross correlation of each window with all others, using sliding windows every 0.1 s during the 30 min of ambient tremor data (Figure 1a) to find pairs that are above a threshold of 3σ, where $\sigma = 1.253 \times$ mean absolute deviation, based on a Gaussian assumption [*Aguiar and Beroza*, 2014]. We later apply the PageRank algorithm to create an LFE template for each of the 10 stations available during this time period. We perform this analysis one station and one component at a time.

We use the LFE stacks created for all components as templates to find other LFEs within continuous data. We use stations where tremor was most clearly observed along all three components for both triggered and ambient tremor. Figure 2a shows the stack for the vertical component for these stations during the ambient tremor.

To test the reliability of our template, we use it to detect LFEs on continuous data for the entire year of 2009 and compare to an existing tremor catalog from *Chao et al.* [2017]. We find a strong correlation between LFE detections found by using our template and tremor detections found by *Chao et al.* [2017] by using envelope cross correlation. Figure 3 shows this comparison for daily, monthly, and yearly scales.

2.2. Triggered Tremor

As mentioned above, tremor is sometimes triggered by teleseismic earthquakes in Taiwan. The 2005 March 28 M_w 8.6 Nias earthquake is one example. *Tang et al.* [2010] used LFEs found manually as templates to detect other LFEs within tremor. We selected data during the time period of this earthquake and focus on 30 min of data where tremor is clearly observed during the passing of the surface waves (Figure 1b). We again apply the PageRank algorithm to the correlations from these 30 min of data and create an LFE template for each of the available stations shown in Figure 2b for the vertical component. We use the new templates to find new detections within the data on each station individually and associate stations as described above.

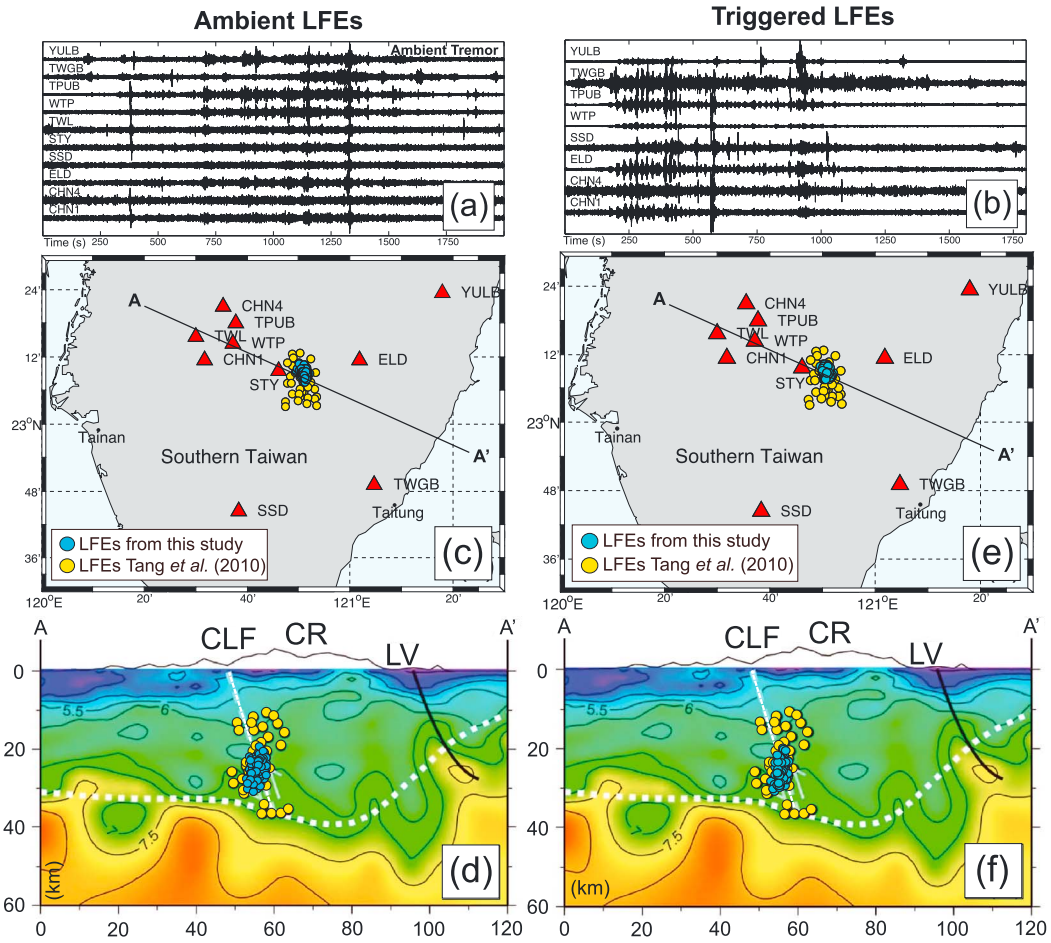

Figure 1. Tremor signal and LFE locations. (a) Thirty minutes of ambient tremor data analyzed in this study for the 10 stations available during 19 January 2009. (b) Thirty minutes of tremor triggered by the 28 March 2005 M_w 8.6 Nias earthquake. (c) LFE epicenters and (d) cross section for LFEs within ambient tremor (blue dots) during 19 January 2009 overlain on the result and Vp model from *Tang et al.* [2010] (yellow dots). (e) LFE epicenters and (f) cross section for LFEs within triggered tremor (blue dots) during 28 March 2009 overlain on *Tang et al.* [2010] (yellow dots). AA' from *Tang et al.* [2010]. The white thick dotted line represents projection of the Chaochou-Lishan Fault (CLF), CR the Central Range, and LV the Longitudinal Valley suture.

3. Comparing the LFE Templates From Ambient and Triggered Tremor

As shown in previous studies, both envelope cross correlations and LFEs found manually within tremor locate ambient and triggered tremor in a similar area [*Chao et al.*, 2012, 2013a; *Chuang et al.*, 2014]. Given their common origin, we compare waveforms to determine if they share the same source mechanism. The LFE templates created from triggered tremor are similar to those created from ambient tremor. This can be seen in Figure 2c as the cross-correlation coefficients of the signals are mostly above 0.5. A couple of stations show a sharper signal for the template of the triggered tremor (i.e., WTP on Figure 2c). Figure 1 shows that ambient tremor has a weaker signal than the triggered tremor, as has been shown for other regions [*Rubinstein et al.*, 2007]. The difference in signal-to-noise ratio that results may explain why the corresponding LFEs appear noisier.

To test this similarity further, we perform template matching by using both templates interchangeably. That is, we use the template created from triggered tremor to detect LFEs within ambient tremor and use the template created from ambient tremor to detect LFEs within triggered tremor. For both types of tremor, we find that most triggered tremor bursts are explained by either set of templates. Given that each station has a different number of detections, we compare both results for each station individually to quantify the overlap using both templates by documenting overlap where both results found a positive detection

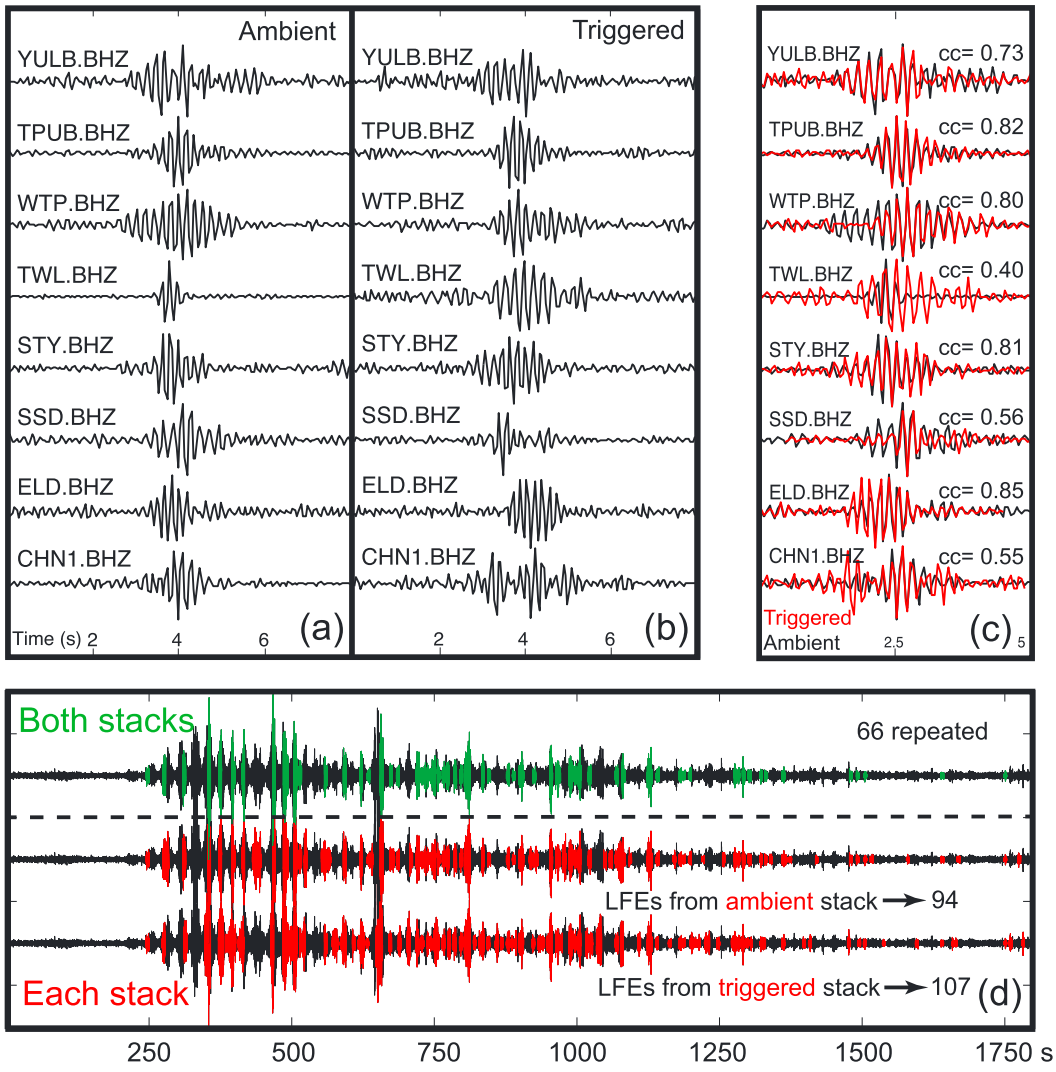

Figure 2. LFE templates and detections during triggered tremor. Vertical components of the (a) LFE stack created by using ambient tremor data in Figure 1a and (b) stack created from triggered tremor data shown in Figure 1b for the best eight stations available. (c) Comparison of template waveforms created from triggered tremor (red) and ambient tremor (black). (d) Detections found by association of stations with detections from the stack of both ambient and triggered tremor analyzed independently (red top and bottom, respectively) compared to the detections that overlap in both analyses (green).

within the same 2 s window. The number of detections found for each component and the degree of detection overlap is listed in Table S1 in the supporting information.

After associating all stations for each case, the stack from triggered tremor revealed a total of 107 detections for a population of 19,920 windows during the 30 min of data. The template from the ambient tremor resulted in a total of 94 detections for the same data set. These results are shown in red in Figure 2d for each stack applied on the triggered tremor data where tremor signal is very clear.

By comparing both sets of detections we find that 66 detections overlap (green, Figure 2d). This means that 62% of the detections found by the triggered tremor template and 70% of the detections found by the ambient tremor template are detections in common. The strong overlap suggests that the LFEs for both events (triggered and ambient) originate from similar sources. We also observe that LFE detections occur mostly during the passing of the triggering surface waves, when amplitudes are largest. Figure 2d also shows that there are no detections just prior to the triggered tremor; however, we see continuing LFE detections after the passing Love waves trigger the initial events.

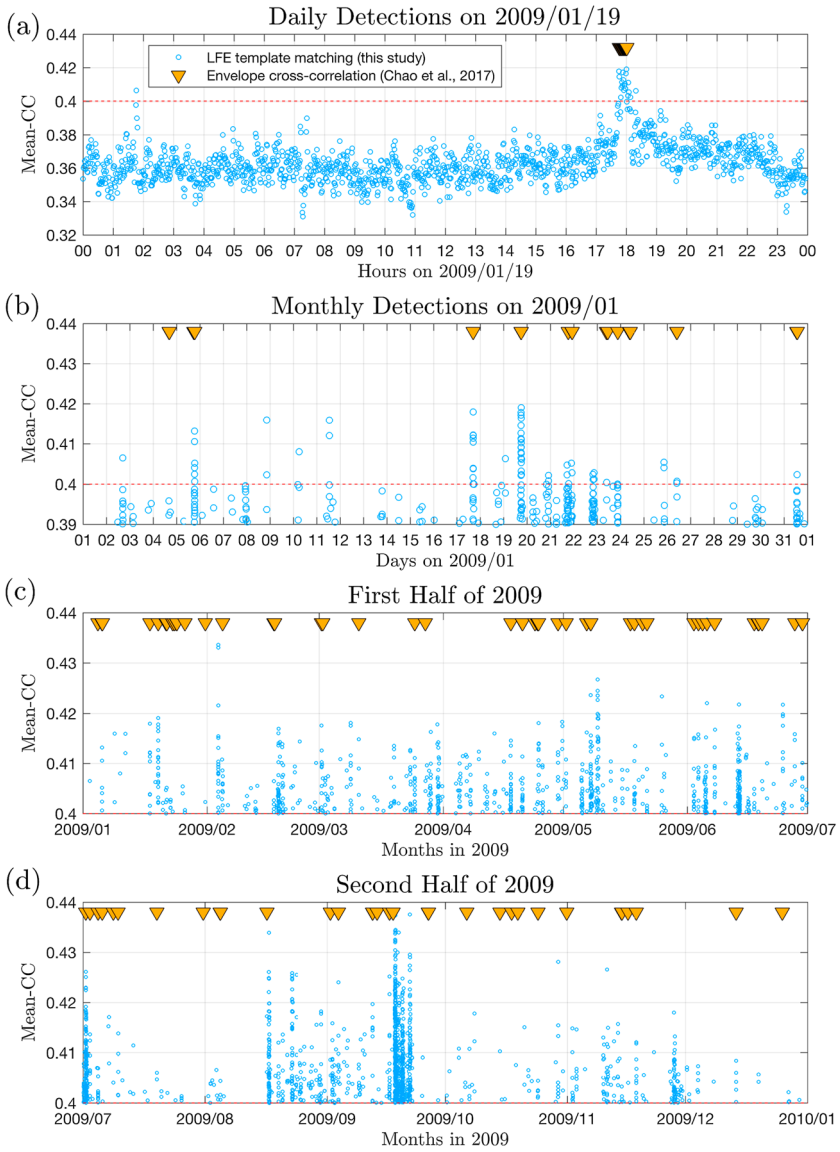

Figure 3. Tremor (with envelope cross-correlation method) and LFE (with template matching method) catalog comparison. (a) Daily, (b) monthly, and (c and d) yearly scales showing the tremor detections from *Chao et al.* [2017] (downward-pointing triangles) compared to detections (blue circles) using the template LFE from ambient tremor.

4. Comparing the LFE Templates to Local Earthquakes

The templates we created from ambient tremor and from triggered tremor represent the *S* wave from the LFEs. After detailed inspection of times ahead of the *S* wave, we were unable to discern unambiguous *P* waves. Given this difficulty, we took a different approach to discern the *P* wave arrivals. The area where tremor has been observed is tectonically active, with many small earthquakes. Using previous knowledge of local seismicity, we take advantage of small earthquakes in close proximity to the tremor. *Shelly et al.* [2006] showed that it is possible to correlate LFEs to earthquakes to determine relative locations. Following this example, we picked a set of earthquakes that sample the area where tremor occurs and that have similar waveforms. These earthquakes have a range of magnitudes M_L 1.5 to 2 and depths from 10 to 36 km. We make this selection by using a simple cross correlation-based agglomerative clustering algorithm, grouping events in a hierarchy. The group of earthquakes selected by the clustering algorithm has 27 events, shown in cyan in Figure 4a.

After filtering earthquake waveforms to match the tremor bandwidth, we compare the LFE template to each of the earthquakes from the cluster to see if the template *S* wave is similar to each earthquake *S* wave. For this,

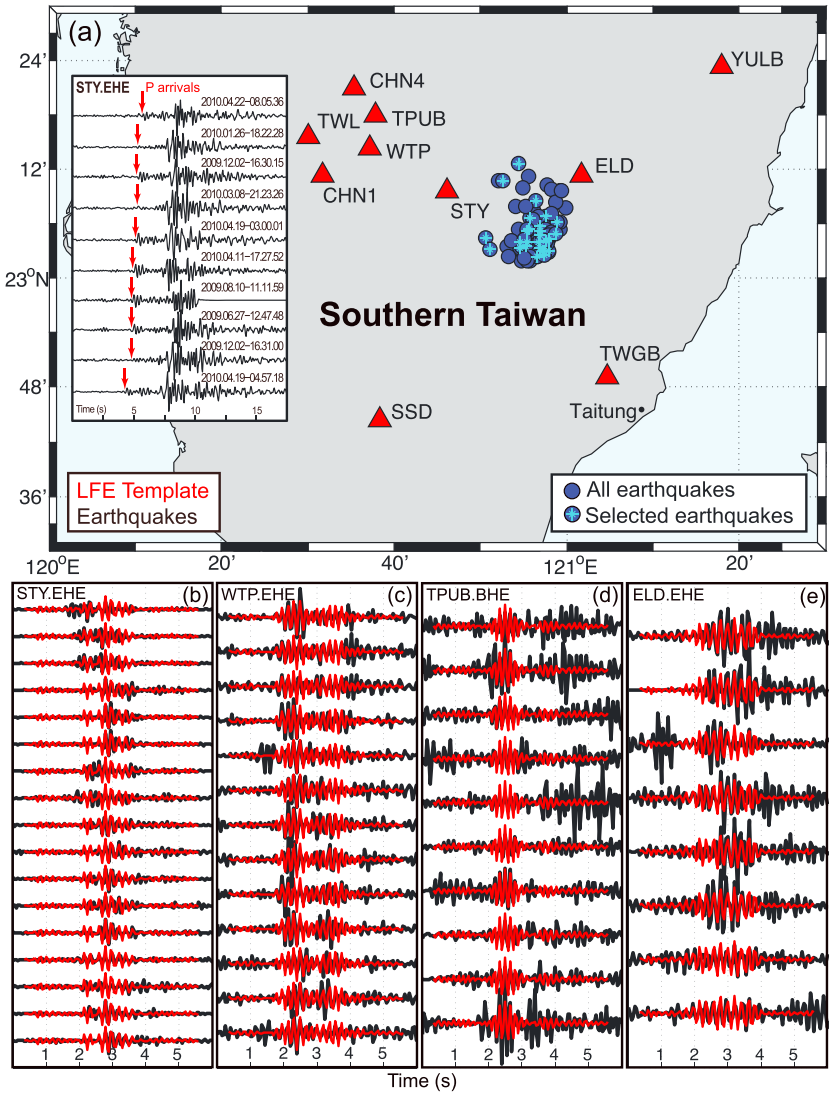

Figure 4. Microearthquake-LFE comparison. (a) Epicenters of 27 earthquakes (cyan stars, examples in inset showing *P* wave arrival), out of a total of 98 events (blue), used to compare with LFE template. (b–e) Clustered earthquakes (black) band-pass filtered and aligned, using cross correlation, with the LFE template (red) from ambient tremor for four different stations with CC > 0.4.

we cross correlate the template with each earthquake and align them based on the cross correlation (Figures 4b–4e). All cross correlations (CC) above 0.4 are shown in Figures 4b–4e for four different stations on one horizontal component. From this we see that the template signal obtained from tremor is very similar to the *S* wave of the clustered earthquakes for most stations. This similarity allows us to use the *P* wave information from the earthquakes to extract the *P* waves of the LFEs and locate them with greater accuracy. From the earthquake data we pick the average *P* wave arrival time for all events and use this to search for the *P* wave on the LFE detections found by using the ambient tremor data.

The LFEs previously found in the ambient tremor can be cross-correlated again at high precision to find the relative arrival times between events. Using the average *P* wave arrival time from the local earthquakes we cross-correlated each LFE detection with all others again, focusing on the time where the *P* wave should be and using a window size of 5.3 s around those times such that we will avoid our assumptions forcing the LFE locations to be similar to the earthquakes. The relative arrival times for the stations used are shown in Table S2.

We find relative *P* wave arrival times by using cross correlation with earthquake *P* waves for the LFE detections prior to the *S* wave arrival on each of the stations. The *P* waves that emerge are in good agreement

with the times listed in Table S2, as shown from the red and yellow dashed lines in Figures S1a and S1b in the supporting information for one of the stations analyzed. These represent the aligned signals to both *S* and *P* waves independently (see also Figures S2–S6). This suggests that the location of the LFEs found during the ambient tremor is close to the earthquakes used to find the *P* wave information of the LFEs. As mentioned previously, the detections used to create the gray scale plots (Figures S1–S6) are detections during the ambient tremor of 19 January 2009. These detections are shown in Figure S1d, which is the result for the associated stations used in the analysis.

We located the detected LFEs by using cross correlation-based relative arrival times for *P* and *S* waves with the double-difference earthquake location method [*Waldhauser and Ellsworth*, 2000]. The resulting locations are shown as blue circles in Figure 1c. These locations form a more compact cluster compared to the previously located LFEs from the 2005 triggered tremor [*Tang et al.*, 2010], but the centroid location is similar for both. The cross section shown in Figure 1d was obtained from *Tang et al.* [2010] and is perpendicular to Taiwan's Central Range. In this cross section we can also see how the locations from our detections are compactly clustered on what appears to be the deep extension of the fault.

Previous studies suggested that the source of the LFEs could be the deep extension of the Chaochou-Lishan Fault [*Tang et al.*, 2010, 2013]. We observe an apparent linear feature in our locations, consistent with this hypothesis. To understand this better we applied the same LFE template to other data from different days where ambient tremor is known to be present and see if we can map this feature more robustly. For this we use data from 28 February 2010 [*Chao et al.*, 2013a, 2017]. We analyzed these 24 h by using the same template created from the ambient tremor from January 2009 presented at the beginning (Figure 2a). We find a total of 1135 detections during the full day of data (Figure S7). This date corresponds to a day where a significant amount of tremor was previously found manually as well as a time of the month where tremor was highly active [*Chao et al.*, 2013a, 2017]. We located these detections as before by using relative arrival times from cross correlation and find a similar clustering to that shown for the ambient tremor of January 2009 (Figures 1c and 1d). These detections show again that locations follow a linear trend between the depths of 20 and 35 km, parallel to the inferred projection of the Chaochou-Lishan Fault [*Kuo-Chen et al.*, 2015; *Rau et al.*, 2012; *Wiltschko et al.*, 2010].

For a direct comparison to the detections found by *Tang et al.* [2010] for the tremor triggered by the 28 March 2005 Nias earthquake, we perform the analysis on the data for this same event. For consistency, we use the template from ambient tremor to find detections during the triggered tremor as well as the same stations as before. We locate these events, again by using relative arrival times from cross correlation (Figure 1e). Like the LFEs from ambient tremor, we find that they are more clustered than the result from *Tang et al.* [2010]. The cross section perpendicular to Taiwan's Central Range from *Tang et al.* [2010] with our locations superimposed shows again a more compact linear feature along the deep extension of the Chaochou-Lishan Fault (Figure 1f), suggesting that it might be the source for the LFEs during the triggered tremor bursts as well.

To estimate the depth error, we perform a bootstrap analysis including all events, with replacement on each iteration of the bootstrap. We do this 100 times and then relocate all 100 realizations of the bootstrap. For the complete set of events we obtain a standard deviation of 1.43 km in depth, so the 95% (2σ) confidence for the LFE depth is just under 3 km. This suggests that our detected LFEs are not deeper than about 30 km, making the correlation with the geologic structure more significant and consistent with the depth of tremor in other continental settings. The locations are consistent with the notion that tremor is occurring on the deep extension of the Chaochou-Lishan Fault, to a depth just above the Moho as found by *Tang et al.* [2010]. To test the consistency of our result further, we compute the theoretical *S-P* times from different depths (Figure S8) for three of the closest stations. We use a 1-D velocity model from *Wu et al.* [2007]. We compare these times (Table S3) with values observed in our data (Table S2) and find the highest consistency with the result for *S-P* times at the depth of 25 km for each station. This consistency agrees with our result given that most of our locations are between 20 and 30 km depth. To show this, using the bootstrap results, we also compute the probability density function of all depths for each event in the analysis (Figure S9). Even though the most probable depths for each event individually vary between 20 and 30 (Figure S9a), we show that the most probable depth for all events in the analysis is around 25–26 km (Figure S9b). These locations are well above the inferred Moho depth [*Tang et al.*, 2010].

5. Discussion and Conclusions

After applying the PageRank algorithm to tremor data from Taiwan, we find that LFE templates created from ambient tremor during January 2009 are very similar to LFE templates within triggered tremor during the passing of the 2005 Nias earthquake surface waves. We also find that by using the LFE templates from either event, we can detect LFEs within most tremor bursts during the triggered tremor of 2005. This similarity between templates strongly suggests that the highly repeating signal recovered from both events is coming from the same source area and that we can recover a reliable LFE signal.

We compared LFE templates from the ambient tremor to local, small earthquakes. After cross-correlating and aligning the templates with the earthquakes, we find that the *S* waves of the templates and earthquakes are very similar. This suggests that the repeating signal we find is generated near the earthquakes and with similar mechanism. To test this further, we used the relative *P* wave arrivals from the local earthquakes to cross-correlate the LFE detections by using this relative time as a focus. We find that the *P* wave arrival times also match the LFE *P* wave arrival and are able to recover a clear arrival during that time for all six stations used in the analysis. This approach helped us obtain *P*- and *S* wave arrivals, which we used to find relative arrival times for locating the LFEs found during ambient tremor.

We apply this approach to find the *P* wave arrival to a longer data set of 24 h during 28 February 2010 where tremor is known to occur, as well as the ambient tremor of 19 January 2009 previously analyzed. In both cases we find that LFEs localize to a more compact cluster compared to previous results of LFEs detected during the triggered tremor of the 28 March 2005 Nias earthquake [*Tang et al.*, 2010]. Within the resolution of the locations, the events that we locate illuminate an apparently planar feature aligned with the downward projection of the Chaochou-Lishan Fault.

Finally, we analyze the tremor triggered by the 28 March 2005 Nias earthquake in a direct comparison to *Tang et al.* [2010] results. By applying the PageRank detection method, we find that LFEs during the tremor triggered by this earthquake follow a more linear feature similar to the LFEs detected during the ambient tremor. This suggests that both types of tremor originate in the same source area with similar mechanism—most likely shear failure on the deeper portion of the Chaochou-Lishan Fault.

Acknowledgments

This work was supported by a Stanford University Fellowship. We utilized the Stanford Center for Computational Earth and Environmental Science for most processing. The short-period CWBSN waveform data (http://gdms.cwb.gov.tw/, permission required) and the broadband BATS data (http://bats.earth.sinica.edu.tw/) were provided by the Taiwan Central Weather Bureau [*Shin et al.*, 2013] and the *Institute of Earth Sciences Academia Sinica in Taiwan* [1996], respectively. We also thank Satoshi Ide for valuable comments that improved the manuscript. K. Chao is supported by the Northwestern Institute for Complex Systems (NICO) and the Center for Optimization and Statistical Learning (OSL) at Northwestern University through the Northwestern Data Science Scholars Fellowship and the Japan Society for the Promotion of Science (JSPS) through awards P12329 and KAKENHI 23244091. Prepared by LLNL under contracts DE-AC52-07NA27344 and LLNL-JRNL-711180.

References

Aguiar, A. C., and G. C. Beroza (2014), PageRank for earthquakes, *Seismol. Res. Lett.*, *85*(2), 344–350.

Brown, J. R., G. C. Beroza, and D. R. Shelly (2008), An autocorrelation method to detect low frequency earthquakes within tremor, *Geophys. Res. Lett.*, *35*, L16305, doi:10.1029/2008GL034560.

Brown, J. R., G. C. Beroza, S. Ide, K. Ohta, D. R. Shelly, S. Y. Schwartz, W. Rabbel, M. Thorwart, and H. Kao (2009), Deep low-frequency earthquakes in tremor localize to the plate interface in multiple subduction zones, *Geophys. Res. Lett.*, *36*, L19306, doi:10.1029/2009GL040027.

Brown, K. M., M. D. Tryon, H. R. DeShon, L. M. Dorman, and S. Y. Schwartz (2005), Correlated transient fluid pulsing and seismic tremor in the Costa Rica subduction zone, *Earth Planet. Sci. Lett.*, *238*(1–2), 189–203.

Chao, K., and K. Obara (2016), Triggered tectonic tremor in various types of fault systems of Japan following the 2012 M_w 8.6 Sumatra earthquake, *J. Geophys. Res. Solid Earth*, *121*, 170–187, doi:10.1002/2015JB012566.

Chao, K., Z. Peng, C. Wu, C.-C. Tang, and C.-H. Lin (2012), Remote triggering of non-volcanic tremor around Taiwan, *Geophys. J. Int.*, *188*(1), 301–324.

Chao, K., Z. Peng, H. Gonzalez-Huizar, C. Aiken, B. Enescu, H. Kao, A. A. Velasco, K. Obara, and T. Matsuzawa (2013a), A global search for triggered tremor following the 2011 M_w 9.0 Tohoku earthquake, *Bull. Seismol. Soc. Am.*, *103*(2B), 1551–1571.

Chao, K., et al. (2013b), Non-volcanic tremor characteristics and tremor generation environment in Taiwan and a case study of their stress interaction with local earthquakes, Abstract S51D-06 presented at 2013 AGU Fall Meeting, San Francisco, Calif, 9–13 Dec.

Chao, K., Z. Peng, Y. J. Hsu, C. Wu, K. Obara, H. C. Pu, K. E. Ching, A. Wech, and P. L. Leu (2017), Temporal variation of tectonic tremor activity in Southern Taiwan around the nearby 2010 M_L 6.3 Jiashian earthquake, *J. Geophys. Res. Solid Earth*, doi:10.1002/2016JB013925, in press.

Chuang, L. Y., K. H. Chen, A. Wech, T. Byrne, and W. Peng (2014), Ambient tremors in a collisional orogenic belt, *Geophys. Res. Lett.*, *41*, 1485–1491, doi:10.1002/2014GL059476.

Frank, W. B., and N. M. Shapiro (2014), Automatic detection of low-frequency earthquakes (LFEs) based on a beamformed network response, *Geophys. J. Int.*, *197*(2), 1215–1223.

Frank, W. B., N. M. Shapiro, V. Kostoglodov, A. L. Husker, M. Campillo, J. S. Payero, and G. A. Prieto (2013), Low-frequency earthquakes in the Mexican Sweet Spot, *Geophys. Res. Lett.*, *40*, 2661–2666, doi:10.1002/grl.50561.

Gomberg, J., J. L. Rubinstein, Z. G. Peng, K. C. Creager, J. E. Vidale, and P. Bodin (2008), Widespread triggering of nonvolcanic tremor in California, *Science*, *319*(5860), 173.

Ide, S., D. R. Shelly, and G. C. Beroza (2007), Mechanism of deep low frequency earthquakes: Further evidence that deep non-volcanic tremor is generated by shear slip on the plate interface, *Geophys. Res. Lett.*, *34*, L03308, doi:10.1029/2006GL028890.

Ide, S., S. Yabe, H.-J. Tai, and K. H. Chen (2015), Thrust-type focal mechanisms of tectonic tremors in Taiwan: Evidence of subduction, *Geophys. Res. Lett.*, *42*, 3248–3256, doi:10.1002/2015GL063794.

Idehara, K., S. Yabe, and S. Ide (2014), Regional and global variations in the temporal clustering of tectonic tremor activity, *Earth Planets Space*, *66*(1), 66.

Institute of Earth Sciences Academia Sinica in Taiwan (1996), Broadband array in Taiwan for seismology, Other/Seismic Networks, doi:10.7914/SN/TW.
Katsumata, A., and N. Kamaya (2003), Low-frequency continuous tremor around the Moho discontinuity away from volcanoes in the southwest Japan, *Geophys. Res. Lett.*, *30*(1), 1020, doi:10.1029/2002GL015981.
Kim, M. J., S. Y. Schwartz, and S. Bannister (2011), Non-volcanic tremor associated with the March 2010 Gisborne slow slip event at the Hikurangi subduction margin, New Zealand, *Geophys. Res. Lett.*, *38*, L14301, doi:10.1029/2011GL048400.
Kuo-Chen, H., F. Wu, W.-L. Chang, C.-Y. Chang, C.-Y. Cheng, and N. Hirata (2015), Is the Lishan fault of Taiwan active?, *Tectonophysics*, *661*, 210–214.
Miyazawa, M., and J. Mori (2005), Detection of triggered deep low-frequency events from the 2003 Tokachi-oki earthquake, *Geophys. Res. Lett.*, *32*, L10307, doi:10.1029/2005GL022539.
Nadeau, R. M., and D. Dolenc (2005), Nonvolcanic tremors deep beneath the San Andreas Fault, *Science*, *307*(5708), 389.
Obara, K., and H. Hirose (2006), Non-volcanic deep low-frequency tremors accompanying slow slips in the southwest Japan subduction zone, *Tectonophysics*, *417*(1–2), 33–51.
Page, L., S. Brin, R. Motwani, and T. Winograd (1999), The PageRank citation ranking: Bringing order to the Web, *Tech. Rep.*, Stanford InfoLab.
Payero, J. S., V. Kostoglodov, N. Shapiro, T. Mikumo, A. Iglesias, X. Pérez-Campos, and R. W. Clayton (2008), Nonvolcanic tremor observed in the Mexican subduction zone, *Geophys. Res. Lett.*, *35*, L07305, doi:10.1029/2007GL032877.
Peng, Z., and K. Chao (2008), Non-volcanic tremor beneath the Central Range in Taiwan triggered by the 2001 M_w 7.8 Kunlun earthquake, *Geophys. J. Int.*, *175*(2), 825–829.
Peng, Z., and J. Gomberg (2010), An integrated perspective of the continuum between earthquakes and slow-slip phenomena, *Nat. Geosci.*, *3*(9), 599–607.
Peterson, C. L., and D. H. Christensen (2009), Possible relationship between nonvolcanic tremor and the 1998–2001 slow slip event, south central Alaska, *J. Geophys. Res.*, *114*, B06302, doi:10.1029/2008JB006096.
Rau, R.-J., J.-C. Lee, K.-E. Ching, Y.-H. Lee, T. B. Byrne, and R.-Y. Chen (2012), Subduction-continent collision in southwestern Taiwan and the 2010 Jiashian earthquake sequence, *Tectonophysics*, *578*, 107–116.
Rogers, G., and H. Dragert (2003), Episodic tremor and slip on the Cascadia Subduction Zone: The chatter of silent slip, *Science*, *300*(5627), 1942–1943.
Rubinstein, J. L., J. E. Vidale, J. Gomberg, P. Bodin, K. C. Creager, and S. D. Malone (2007), Non-volcanic tremor driven by large transient shear stresses, *Nature*, *448*(7153), 579–582.
Shelly, D. R., G. C. Beroza, S. Ide, and S. Nakamula (2006), Low-frequency earthquakes in Shikoku, Japan, and their relationship to episodic tremor and slip, *Nature*, *442*(7099), 188–191.
Shelly, D. R., G. C. Beroza, and S. Ide (2007a), Complex evolution of transient slip derived from precise tremor locations in western Shikoku, Japan, *Geochem. Geophys. Geosyst.*, *8*, Q10014, doi:10.1029/2007GC001640.
Shelly, D. R., G. C. Beroza, and S. Ide (2007b), Non-volcanic tremor and low-frequency earthquake swarms, *Nature*, *446*(7133), 305–307.
Shin, T. C., C. H. Chang, H. C. Pu, H. W. Lin, and P. L. Leu (2013), The geophysical database management system in Taiwan, *Terr. Atmos. Ocean. Sci.*, *24*(1), 11–18.
Shin, T.-C., and T.-l. Teng (2001), An overview of the 1999 Chi-Chi, Taiwan, earthquake, *Bull. Seismol. Soc. Am.*, *91*(5), 895–913.
Sun, W. F., Z. Peng, C. H. Lin, and K. Chao (2015), Detecting deep tectonic tremor in Taiwan with a dense array, *Bull. Seismol. Soc. Am.*, *105*(3), 1349–1358.
Tang, C.-C., Z. Peng, K. Chao, C.-H. Chen, and C.-H. Lin (2010), Detecting low-frequency earthquakes within non-volcanic tremor in Southern Taiwan triggered by the 2005 M_w 8.6 Nias earthquake, *Geophys. Res. Lett.*, *37*, L16307, doi:10.1029/2010GL043918.
Tang, C.-C., Z. Peng, C.-H. Lin, K. Chao, and C.-H. Chen (2013), Statistical properties of low-frequency earthquakes triggered by large earthquakes in Southern Taiwan, *Earth Planet. Sci. Lett.*, *373*, 1–7.
Waldhauser, F., and W. L. Ellsworth (2000), A double-difference earthquake location algorithm: Method and application to the northern Hayward fault, *Bull. Seismol. Soc. Am.*, *90*(6), 1353–1368.
Wiltschko, D. V., L. Hassler, J.-H. Hung, and H.-S. Liao (2010), From accretion to collision: Motion and evolution of the Chaochou Fault, Southern Taiwan, *Tectonics*, *29*, TC2015, doi:10.1029/2008TC002398.
Wu, F. T., Z. E. Ross, D. Okaya, Y. Ben-Zion, C.-Y. Wang, H. Kuo-Chen, and W.-T. Liang (2016), Dense network, intense seismicity and tectonics of Taiwan, *Tectonophysics*, *692*, 152–163.
Wu, Y.-M., C.-H. Chang, L. Zhao, J. B. H. Shyu, Y.-G. Chen, K. Sieh, and J.-P. Avouac (2007), Seismic tomography of Taiwan: Improved constraints from a dense network of strong motion stations, *J. Geophys. Res.*, *112*, B08312, doi:10.1029/2007JB004983.
Yu, S.-B., H.-Y. Chen, and L.-C. Kuo (1997), Velocity field of GPS stations in the Taiwan area, *Tectonophysics*, *274*(1–3), 41–59.